8-17-2007

Observation of type-I and type-II excitons in strained Si/SiGe quantum-well structures

K. Y. Wang
National Taiwan University

W. P. Huang
National Taiwan University

H. H. Cheng
National Taiwan University

Greg Sun
University of Massachusetts Boston, greg.sun@umb.edu

R. A. Soref
Air Force Research Laboratory, Hanscom Air Force Base

See next page for additional authors

Observation of type-I and type-II excitons in strained Si/SiGe quantum-well structures

K. Y. Wang, W. P. Huang, H. H. Cheng, G. Sun, R. A. Soref et al.

Citation: Appl. Phys. Lett. **91**, 072108 (2007); doi: 10.1063/1.2771094
View online: http://dx.doi.org/10.1063/1.2771094
View Table of Contents: http://apl.aip.org/resource/1/APPLAB/v91/i7
Published by the American Institute of Physics.

Observation of type-I and type-II excitons in strained Si/SiGe quantum-well structures

K. Y. Wang, W. P. Huang, and H. H. Cheng[a)]
Center for Condensed Matter Sciences and Graduate Institute of Electronics Engineering, National Taiwan University, Taipei, 106 Taiwan, Republic of China

G. Sun
Department of Physics, University of Massachusetts, Boston, Massachusetts 02125

R. A. Soref
Sensors Directorate, Air Force Research Laboratory, Hanscom AFB, Massachusetts 01731

R. J. Nicholas
Department of Physics, University of Oxford, Oxford OX1 3PU, United Kingdom

Y. W. Suen
Department of Physics, National Chung Hsing University, Taichung 402, Taiwan and National Nano Device Laboratories, Hsinchu, Taiwan 30078, Republic of China

(Received 15 June 2007; accepted 22 July 2007; published online 17 August 2007)

The authors report photoluminescence (PL) measurement on a series of Si/SiGe quantum-well structures that had different internal strain distributions. When each sample was placed in a high magnetic field, the field-dependent energy shift of the relevant PL peaks revealed either type-I or type-II exciton formation depending on the strain distribution. This observation is in agreement with theoretical modeling. The present investigation shows that type-I band alignment—desired for electroluminescent devices—can be achieved by strain engineering. © *2007 American Institute of Physics*. [DOI: 10.1063/1.2771094]

Strained $Si/Si_{1-x}Ge_x$ heterostructures grown on relaxed $Si_{1-x}Ge_x$ buffer layers on Si substrates have attracted a great deal of attention in recent years for their applications in both electronic and photonic devices. It has been generally accepted that holes in these heterostructures experience potential wells in the $Si_{1-x}Ge_x$ layer and barriers in Si. The situation in conduction band (CB), however, is rather obscure under the influence of alloying and strain effects, resulting in some uncertainty on whether type-I or type-II band alignment is formed in a given multiple quantum well (MQW) structure.[1–5] However, being able to precisely determine the type of alignment has a direct impact on device properties, e.g., type-I alignment offers a larger band-to-band oscillator strength than type II; thus a stronger radiative emission efficiency is expected from type-I devices. We demonstrate in this study that the strain can be utilized to manipulate band alignment.

We report the magnetoluminescence (ML) study on two set of $Si/Si_{1-x}Ge_x$ MQW structures with different strain distributions. The two sets of samples exhibited very different magnetic-field-dependent energy shifts in the ML measurement. Samples with strain present only in Si layers show a large shift consistent with the conventional type-II excitons. For samples with strain in both Si and SiGe layers, a small negative shift is observed reflecting a rather different carrier effective mass involved in the optical transition. From the analysis of strain-induced band shifting and modeling of these energy shifts, formation of type-I excitons has been obtained.

The samples were grown by solid source molecular beam epitaxy on Si (001) wafers. All samples consist of (a) a thin layer of Si grown at low temperature, (b) a thick buffer layer of $Si_{1-x}Ge_x$ (4000 Å) as a virtual substrate, and (c) ten periods of $Si/Si_{1-x}Ge_x$ QWs. Alloy compositions and layer widths are determined by x-ray diffraction measurement and transmission electron microscopy. The sample structures are summarized in Table I. The major difference of the two sets of samples is the different degrees of strain relaxation (R) in the $Si_{1-x}Ge_x$ buffer layer. The details of the growth technique are described in Ref. 6. The strain distributions in the QW regions of these samples depend on the degree of relaxation of the SiGe buffer layers. For high Ge samples ($x=40\%$), $Si_{0.6}Ge_{0.4}$ buffer layers are fully relaxed. As a result, the $Si_{0.6}Ge_{0.4}$ layers in the QW structure are also fully relaxed with only Si layers strained due to the lattice mismatch. For low Ge samples ($x=15\%$), buffer layers are only partially relaxed and consequently, Si and $Si_{0.85}Ge_{0.15}$ layers have tensile and compressive in-plane strain, respectively. These different strain situations have been determined by Raman measurement and the results are listed in Table I.

We have conducted ML measurement on these samples at liquid helium temperature in high magnetic fields up to 15 T. Luminescence was excited by an optical fiber using a solid-state laser ($\lambda=532$ nm) with intensity levels around 1 mW/cm^2. The free-space emission was collected by a fiber bundle, dispersed by a half-meter spectrometer, and detected by a thermoelectrically cooled InGaAs detector. The measurements were performed in a Faraday configuration.

Photoluminescence (PL) spectra at zero magnetic field from the two samples N1 and N3 are plotted in Fig. 1. Several features are resolved in the energy range between 0.75 and 1.2 eV. On the high-energy side of the spectra for all

a)Author to whom correspondence should be addressed; electronic mail: hhcheng@ntu.edu.tw

TABLE I. Summary of sample structures and the transition energy of the no-phonon (NP) lines. R is the degree of relaxation of the SiGe buffer layer. A negative value of the Δ_4 offset indicates that the band edge of SiGe layer lies below the Si layer forming a type-I structure.

Sample	Ge (%)	Si/SiGe width (Å)	R	Offset (Δ_2/Δ_4) (eV)	Offset (HH/LH) (eV)	NP (eV)
N1	40	100/75	1	0.24/−0.013	0.183/0.096	0.794
N2	40	100/115	1	0.24/−0.013	0.183/0.096	0.785
N3	15	50/65	0.1	0.071/−0.023	0.103/0.007	1.053
N4	15	55/45	0.1	0.071/−0.023	0.103/0.07	1.066

samples, a set of bulk Si-related transitions is observed at peak energies of 1.151, 1.136, and 1.092 eV, corresponding to the no phonon (NP), transverse acoustic (TA), and transverse optical (TO) mode phonon replicas. In the low energy regime, several PL lines are observed, and the peak positions depend on the Ge composition of the sample. For sample N1, a broad PL line at a peak energy of 0.854 eV is observed labeled by D2, shown in Fig. 1(a). This is attributed to the transitions associated with the dislocations (D2 band) that are developed at the $Si/Si_{0.6}Ge_{0.4}$ interfaces due to the large lattice mismatch between Si and $Si_{0.6}Ge_{0.4}$. Superimposed upon the low energy shoulder of this broad peak are NP and TA transitions from the QW region. (These features are extremely weak, but become better resolved as the magnetic field is applied. For sample N3, well resolved NP, TA, and TO replicas from the QW region can be identified as marked by the solid arrows in Fig. 1(b). In addition to these main features, a weak feature appears at the high energy shoulder of the NP line. This is attributed to the combination of small well width and Ge composition fluctuation in the QWs. Around the TA-phonon replica, another weak feature is also observed, possibly due to the different modes of Si–Si, Si–Ge, and Ge–Ge vibrations. These exciton transitions are listed in Table I.

A family of ML spectra in the energy window of the QW transition from the two samples N1 and N3 are plotted in Fig. 2. The two originally weak QW exciton transitions from sample N1 become stronger because of the increase of in-plane oscillator strength due to the reduction of the cyclotron orbit under the applied magnetic field. The transitions continue to shift to higher energy as the magnetic field increases as marked by the dotted arrow line, reaching ~10 meV at the highest magnetic field $B=15$ T. For sample N3, the QW transitions move slightly towards lower energy reaching a negative value of ~1 meV at $B=14$ T. The energy shift of the NP line of the two samples is plotted in Fig. 3. The ML spectra for sample N2 (N4) with the same strain distribution as N1 (N3) show a similar shifting behavior as N1 (N3). These different shifting behaviors can be explained with the cyclotron energy and the Zeeman effect.[7] As the applied magnetic field increases, the exciton transitions undergo a shift towards higher energy by the amount of cyclotron energy which can be approximated as $\hbar\omega=eB/\mu_{\|}$, where the reduced in-plane effective-mass $\mu_{\|}$ is related to the in-plane effective mass of electrons ($m_e^{\|}$) and holes ($m_h^{\|}$) by $1/\mu_{\|}=1/m_e^{\|}+1/m_h^{\|}$. This shift of ground-state exciton transition energy is compensated by the Zeeman effect which splits the spin states of the carriers by $\Delta_{S\text{-}T}=-g\mu_B B$, where the μ_B is the Bohr magneton and g the Landé g factor. Since the Zeeman effect is relatively weak (Zeeman splitting of bulk SiGe is about −1 meV at 14 T), the large difference in the shifting behavior of the two sets of samples can only be explained by the rather different in-plane effective masses of the carriers through the cyclotron energy.

We now perform energy band analysis under the influence of strain in order to reveal the origin of these exciton transitions. Our approach is based on the model solid theory[8] with the alignment of the average valence band offset[9] between the two layers and the compositional dependence of the $Si_{1-x}Ge_x$ band gap[10–12] followed by the effect of strain that moves and splits various CB and VB edges.[8] For the $Si/Si_{0.6}Ge_{0.4}$ samples, where $Si_{0.6}Ge_{0.4}$ layers are relaxed with no appreciable strain, there is no splitting of the Δ valleys in $Si_{0.6}Ge_{0.4}$ layers. The Δ_2 band, therefore, forms QWs in Si layers and barriers in $Si_{0.6}Ge_{0.4}$ layers. The tensile strain in Si layers will also split the HH and light hole (LH) bands with LH sitting above HH. Both LH and HH bands form QWs in $Si_{0.6}Ge_{0.4}$ layers and barriers in Si layers. The effect

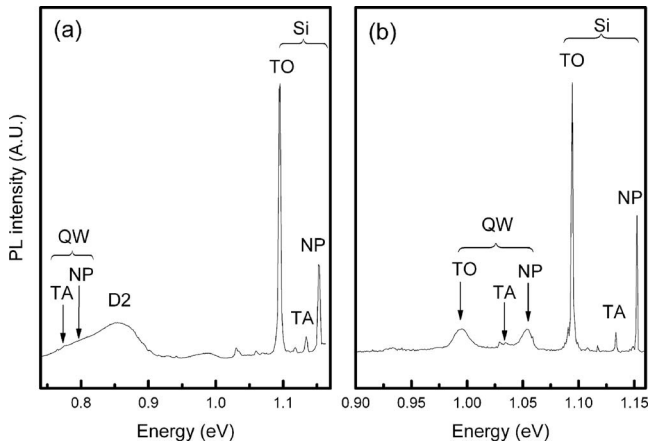

FIG. 1. PL spectra of samples N1 (a) and N3 (b) at zero magnetic field.

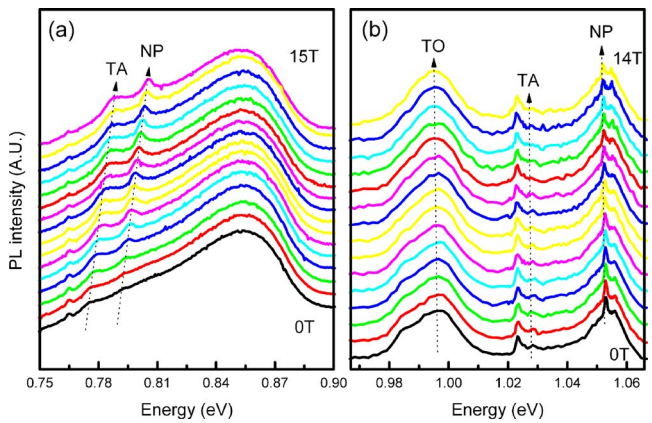

FIG. 2. (Color online) ML spectra for samples N1 (a) and N3 (b).

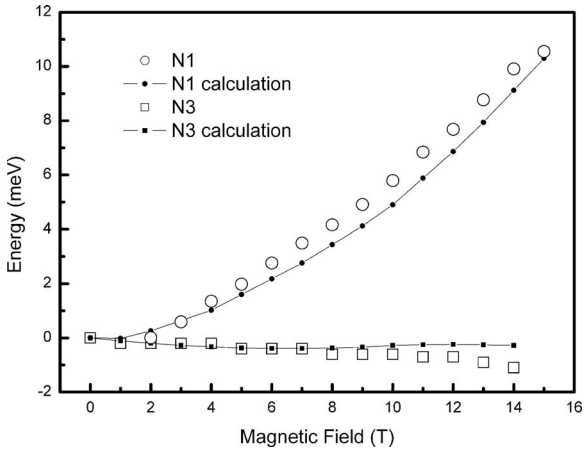

FIG. 3. Experimental (open symbols) and calculated (full symbols) energy shifts of the QW NP peaks plotted as a function of magnetic field for samples N1 and N3.

of quantum confinement will lift ground-state HH above that of LH in $Si_{0.6}Ge_{0.4}$ layers. As result, a type-II band alignment is formed between Δ_2 and HH band edges in $Si/Si_{0.6}Ge_{0.4}$ samples. The ground-state excitons are therefore formed by Δ_2-band electrons and HHs in a type-II situation where the electrons are localized in Si and HHs in $Si_{0.6}Ge_{0.4}$. For $Si/Si_{0.85}Ge_{0.15}$ samples, while Si layers are still under tensile strain, $Si_{0.85}Ge_{0.15}$ layers are simultaneously under compressive strain which splits Δ_2 and Δ_4 bands in the opposite direction. The Δ_2 band edge rises in energy and Δ_4 band edge falls in energy. The different strains in Si and $Si_{0.85}Ge_{0.15}$ layers will also split HH and LH bands in the opposite directions. Within $Si_{0.85}Ge_{0.15}$ layers, the HH band edge is higher than that of LH. The lowest CB is now the Δ_4 band with $Si_{0.85}Ge_{0.15}$ QWs and Si barriers, and the highest VB is the HH band also with $Si_{0.85}Ge_{0.15}$ as QWs, leading to a type-I band alignment where both electrons and holes are confined in $Si_{0.85}Ge_{0.15}$ layers. The ground-state excitons are therefore formed by Δ_4-band electrons and HHs. Using the parameters from Ref. 9 and the sample structures listed in Table I, the band offsets for both the CB and VB are calculated and the results are summarized in Table I.

With these band structures, we can now calculate the exciton transition energies using a self-consistent model that takes into account of Coulomb interaction. The exciton Hamiltonian in cylindrical coordinates (ρ, ϕ, z) can be written as[13]

$$H = \left[-\frac{\hbar^2}{2m_e^{\perp}}\frac{\partial^2}{\partial z_e^2} + V_e \right] + \left[-\frac{\hbar^2}{2m_h^{\perp}}\frac{\partial^2}{\partial z_h^2} + V_h \right] + \frac{e^2B^2}{8\mu_{\parallel}}\rho^2,$$
$$- \frac{\hbar^2}{\mu_{\parallel}}\left[\frac{1}{\rho}\frac{\partial}{\partial\rho}\rho\frac{\partial}{\partial\rho} + \frac{1}{\rho^2}\frac{\partial^2}{\partial\phi^2} \right] - \frac{e^2}{4\pi\varepsilon_0\varepsilon}\frac{1}{\sqrt{\rho^2 + (z_e - z_h)^2}}$$

where $m_e^{\perp}$ and $m_h^{\perp}$ are effective masses of electrons and holes in the perpendicular direction (z), and V_e and V_h are the potentials for electrons and holes, respectively. For Δ_2 electrons $m_e^{\parallel}=0.19m_0$ and $m_e^{\perp}=0.92m_0$, and for Δ_4 electrons $m_e^{\parallel}=0.42m_0$ and $m_e^{\perp}=0.19m_0$. The HH effective masses are derived from the Luttinger parameters[9] using a linear interpolation between Si and Ge. The three-dimensional exciton Hamiltonian is solved by the variational method.[14] The correction of the Zeeman effect has been taken into account using the experimental value[7] of $g=2$ which is mainly responsible for the negative shift observed in sample N3. The magnetic-field-dependent energy shift is obtained by taking the difference in exciton transition energies calculated with or without the magnetic-field term in the Hamiltonian. The calculated result agrees quite well with our measurement, as shown in Fig. 3 for samples N1 and N3. The amount of shifting between the two samples is quite different. For sample N1 with excitons formed by Δ_2 electrons and HHs, the shift is rather significant. For sample N3 with excitons formed by Δ_4 electrons and HHs, the shift is quite small. Since both samples have HHs as one type of carriers forming the ground-state excitons, the dramatic difference exhibited in the shifting between the two samples should be attributed to the different in-plane effective masses between the Δ_2 and Δ_4 electrons. The small in-plane effective mass of Δ_2 electrons gives rise to large NP-line energy shift in sample N1, while the opposite is true for sample N3 in which the excitons are formed by HHs and Δ_2 electrons with large in-plane effective mass. The correction of Zeeman effect has also been included in the calculation.

Because of the rather small CB offset in our type-I $Si/Si_{0.85}Ge_{0.15}$ samples, any variation of parameters used in the band structure analysis can lead to uncertainty in determining the type of band alignment discussed above. Therefore, we provide the following argument to remove any ambiguity regarding the accuracy of our model upon which the claim of type-I alignment is made. From the shift of ML peaks, we have identified that the electrons that form the excitons are indeed from Δ_4 band in $Si/Si_{0.85}Ge_{0.15}$ samples. If the Δ_4 band formed a type-II alignment with HH band, i.e., electrons are confined in Si layers, then we should have observed in ML measurement exciton transitions with electrons from Δ_2 band which sits lower than Δ_4 band in tensile strained Si layers. The fact that these exciton transitions are from Δ_4-band electrons further suggests that not only type-I alignment is formed between the Δ_4 and HH band but also that the Δ_4 band is the lowest CB.

The present investigation shows that the band alignment in $Si/Si_{1-x}Ge_x$ QWs is sensitive to strain distribution. With a proper strain manipulation, it is possible to form a type-I band alignment with larger oscillator strength for more efficient infrared emission from a silicon-based Si/SiGe light-emitting diode.

Financial support from the National Science Council (Taiwan) and AFOSR (USA) is acknowledged.

[1]Michele Virgilio and Giuseppe Grosso, J. Phys.: Condens. Matter **18**, 1021 (2006).
[2]R. People and J. C. Bean, Appl. Phys. Lett. **48**, 538 (1986).
[3]M. M. Rieger and P. Vogl, Phys. Rev. B **48**, 14276 (1993).
[4]D. C. Houghton, G. C. Aers, S. R. Eric Yang, E. Wang, and N. L. Rowell, Phys. Rev. Lett. **75**, 866 (1995).
[5]M. L. W. Thewalt, D. A. Harrison, C. F. Reinhart, and J. A. Wolk, Phys. Rev. Lett. **79**, 269 (1997).
[6]W. S. Tan, H. H. Cheng, V. I. Mashanov, Y. F. Wong, and C. T. Chia, Appl. Phys. Lett. **88**, 162111 (2006).
[7]H. Heckler, D. Kovalev, and G. Polisski, Phys. Rev. B **60**, 7718 (1999).
[8]Chris G. Van de Walle, Phys. Rev. B **39**, 1871 (1989).
[9]D. J. Paul, Semicond. Sci. Technol. **19**, R75 (2004).
[10]S. Richard, F. Aniel, G. Fishman, and N. Cavassilas, J. Appl. Phys. **94**, 1795 (2003).
[11]D. J. Robbins, L. T. Canham, S. J. Barnett, A. D. Pitt, and P. Calcott, J. Appl. Phys. **71**, 1407 (1992).
[12]R. People, Phys. Rev. B **32**, 1405 (1985).
[13]C. Penn, F. Schaffler, and G. Bauer, Phys. Rev. B **61**, 13055 (2000).
[14]H. H. Cheng, S. T. Yen, and R. J. Nicholas, Phys. Rev. B **62**, 4638 (2000).